

## Excitation energy dependency of the low-energy fission dynamics: Probing through prompt gamma-ray spectroscopy

Aniruddha Dey<sup>1,2,\*,\*\*</sup>, D. C. Biswas<sup>1,3</sup>, A. Chakraborty<sup>2,\*\*\*</sup>, and S. Mukhopadhyay<sup>1,3</sup>

<sup>1</sup>Nuclear Physics Division, Bhabha Atomic Research Centre, Mumbai 400 085, India

<sup>2</sup>Department of Physics, Siksha Bhavana, Visva-Bharati University, Santiniketan, West Bengal 731 235, India

<sup>3</sup>Homi Bhabha National Institute, Anushaktinagar, Mumbai 400 094, India

**Abstract.** Fission Fragment Spectroscopy (FFS) technique has been utilized to make simultaneous measurements of both the relative charge and mass yield distributions of even-even fission fragments produced from the fission of  $^{236}\text{U}$  at two different excitation energies,  $E_{ex}$ . The necessary analysis has been carried out on the measured yield distributions by employing the Multimodal Random Neck Rupture Model (MM-RNRM). The relative contribution of two different types of asymmetric mode of fission – Standard I and Standard II has been extracted at  $E_{ex} = 6.5$  and  $21.5$  MeV. An attempt has been made to study the evolution of these two asymmetric fission modes with respect to the values of  $E_{ex}$  of the concerned fissioning system at low-excitation regime. The probable evidence, although at the primitive stage, for an oscillatory behavior of the relative contributions of different low-energy fission modes with increasing values of  $E_{ex}$  has been presented.

### 1 Introduction

The complex process of nuclear fission was discovered more than eight decades ago, and still, it is an active area of research both in the fields of experiment and theory. In a typical fission process, a large-scale collective rearrangement of nucleonic matter takes place within a very short interval of time typically of the order of  $10^{-21}$  seconds, and subsequently several fission fragment nuclei are produced [1]. Due to such complexity, there exist several issues related to the underlying fission dynamics that are yet to be resolved satisfactorily. Since early 1960s, one of the most prominent and well-known experimental observables of fission process has been the existence of the asymmetric and symmetric mass yield distributions [2]. This has ultimately led to the concept for the existence of different fission modes in the potential energy surface (PES) valley of the concerned fissioning system [3]. In Ref.[4], Brosa *et al.* proposed one of the most successful theoretical approaches for interpreting the existence of multiple fission modes based on the Multimodal Random-Neck Rupture Model (MM-RNRM). According to this model, the fissioning nucleus encounters multiple bifurcation points in the PES due to the existence of shell structure effects. These bifurcation points lead to the development of different fission modes corresponding to different barriers. At lower excitation energies, the lighter actinides exhibit primarily three distinct fission modes, namely – two asymmetric modes: standard I (S1), standard II (S2), and one

symmetric superlong (SL) mode. The symmetric SL mode is due to the classical behavior of the fissioning nucleus based on the Liquid Drop Model (LDM). However, the occurrence of the two asymmetric S1 and S2 fission modes have been attributed to the presence of two neutron shell closures, the spherical one corresponding to  $N = 82$ , and the deformed one corresponding to  $N = 88$  [4].

Till now, several studies have been carried out to investigate the existence of the aforesaid different low-energy fission modes. However, the comprehensive knowledge regarding the influence of the excitation energy ( $E_{ex}$ ) and angular momentum ( $L$ ) in controlling the dynamics of different fission modes is yet to be obtained. Indeed, one of the first such attempt was made by Brosa *et al.* [4] to study the influence of excitation energy for populating the ‘Brosa’ modes of fission in  $^{236}\text{U}$  at lower  $E_{ex}$  values ( $E_{ex} < 12$  MeV). Interestingly, the theoretical estimation of Ref.[4] indicated an increase in the relative probability of S1 mode unlike that of S2 mode with  $E_{ex}$  [5]. On the other hand, the work of Ref.[6] indicated a constant steady increase of relative probability of S2 mode in the same energy range, and a significant contribution of S1 mode persists up to  $E_{ex} \sim 25$  MeV for the reaction,  $^{238}\text{U}(n,f)$ . But according to the Wahl’s predicted systematics [7], the contribution from S1 fission mode must vanish beyond 25 MeV due to the dilution of shell effect in  $^{132}\text{Sn}$ . The complexity further gets enhanced due to the significant and simultaneous influence of the multichance fission (MCF) phenomena on the underlying fission modes [8]. However, no significant influence of MCF was found in the work of Ref.[9] for the reaction,  $^{232}\text{Th}(p,f)$ . In fact, a nearly steady yield from S1 mode was reported up to  $E_{ex} < 26$  MeV. In contrary, an indication for the oscillatory behavior was

\*e-mail: deyaniruddha@jinr.ru

\*\*Present address: Flerov Laboratory of Nuclear Reactions, Joint Institute for Nuclear Research, Dubna 141 980, Russia.

\*\*\*e-mail: anagha.chakraborty@visva-bharati.ac.in

found to exist in the yield contributions corresponding to S1 and S2 fission modes with increasing value of  $E_{ex}$  for the low-energy fission reaction,  $^{238}\text{U}(n,f)$  [10]. Therefore, the exact nature of variation of different low-energy fission modes with  $E_{ex}$  is still largely questionable and undetermined. The recent study based on the low-energy fissioning system,  $^{232}\text{Th}(p,f)$  has again rejuvenated the argument, and provided clear evidence of oscillatory pattern in the yields and mass peaks corresponding to the two asymmetric, S1 and S2 fission modes up to  $E_{ex} \sim 35$  MeV [11]. Hence, an extensive investigation is very much desirable to understand the dynamics of low-energy fission modes. In this context, a modest attempt has been made through the present investigation by using the fission fragment spectroscopy technique [12–14].

The primary motivation of the present investigation is to study the dependency of  $E_{ex}$  on the various low-energy fission modes in  $^{236}\text{U}$ . With this motivation, the characteristics of different asymmetric and symmetric fission modes have been studied by measuring the relative yields of these coexisting modes in  $^{236}\text{U}$  at two different values of  $E_{ex}$ . Based on the MM-RNRM, detailed multimodal analysis of the measured profiles of both the relative charge and mass yield distributions for the even-even fission fragments have been carried out.

## 2 Experimental details

The present study deals with the fissioning compound nucleus,  $^{236}\text{U}^*$  populated through two different experiments at two different values of  $E_{ex}$ . The first experiment,  $^{235}\text{U}(n_{th},f)$  was performed during the EXILL campaign at the PF1B neutron beamline of the high-flux reactor facility at the Institut Laue-Langevin (ILL), Grenoble, France. A stacked  $\text{UO}_2$  target of thickness  $\approx 600 \mu\text{g}/\text{cm}^2$  was bombarded with a collimated thermal-neutron beam. The deexciting  $\gamma$  rays from the various fission fragments were detected using the EXILL array [15]. The array was comprised of eight EXOGAM Clover detectors, six large coaxial detectors from GASP, and the two clover detectors from the ILL. A triggerless, digital data acquisition system based on 14 bit 100 MHz CAEN digitizer was used to collect the spectroscopic data in  $\gamma\gamma$  and  $\gamma\gamma\gamma$  coincidence formats. Both the  $\gamma\gamma$  and  $\gamma\gamma\gamma$  coincidence data were sorted using a coincidence prompt time window of 200 nano second. Further details of the experimental set up can be found in Refs. [12, 15]. The second experiment following the reaction,  $^{232}\text{Th}(\alpha,f)$  was performed at Variable Energy Cyclotron Centre (VECC), Kolkata, India, using the Indian National Gamma Array (INGA) spectrometer [16] comprised of six Compton suppressed HPGe Clover detectors and one LEPS detector. A self-supporting  $^{232}\text{Th}$  target of thickness  $\approx 25 \text{ mg}/\text{cm}^2$  was bombarded with 30 MeV  $\alpha$  beam delivered by K-130 cyclotron. Digital Signal Processing (DSP) based data acquisition system, consisting of 250 MHz 12-bit PIXIE-16 digitizer manufactured by XIA, LLC (USA) and running on a firmware conceptualized by UGC-DAE CSR, Kolkata Centre, was used to acquire time-stamped, Compton suppressed  $\gamma\gamma$  coincidence data. Further experimental details regarding the

INGA campaign at VECC can be found in Ref.[16]. The offline spectral analysis of the prompt coincidence data acquired from both the experiments was carried out using RADWARE [17] and Tv [18] software packages.

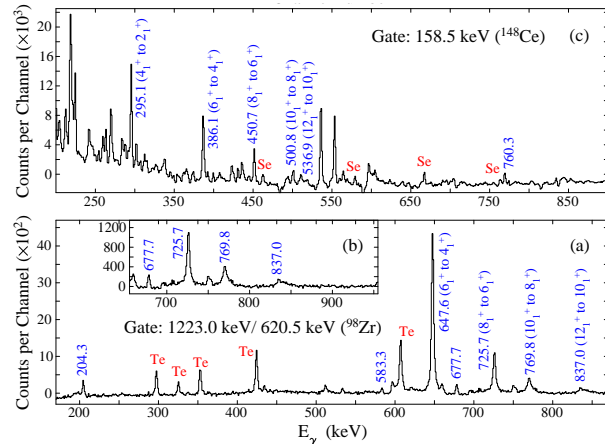


**Figure 1.** (a) Representative double gated coincidence spectrum generated by applying gates on 1223.0 keV,  $2_1^+ \rightarrow 0_1^+$  and 620.5 keV,  $4_1^+ \rightarrow 2_1^+$  transitions of  $^{98}\text{Zr}$ . Part of the spectrum (a) has been zoomed in and shown as the inset, (b). (c) Representative single gated coincidence spectrum generated by applying gate on 158.5 keV,  $2_1^+ \rightarrow 0_1^+$  transition of  $^{148}\text{Ce}$ . The spectra have been generated using the data acquired from the experiment with the  $^{235}\text{U}(n_{th},f)$  reaction.

## 3 Analysis and Results

The first experiment,  $^{235}\text{U}(n_{th},f)$  produced the fissioning compound nucleus,  $^{236}\text{U}$  at an excitation energy ( $E_{ex}$ ) of 6.5 MeV [12]. The same compound nucleus was again produced in the second experiment following the reaction,  $^{232}\text{Th}(\alpha,f)$  at  $E_{ex} = 21.5$  MeV [16]. The high-statistics prompt  $\gamma$  ray coincidence data from both the experiments have been utilized to extract the relative isotopic yield distributions of the even-even fission fragments. The representative  $\gamma\gamma\gamma$  and  $\gamma\gamma$  coincidence spectra obtained from the first experiment have been shown in figure 1. The spectrum shown in figure 1(a),(b) has been generated by applying the gates on 1223.0 keV,  $2_1^+ \rightarrow 0_1^+$  and 620.5 keV,  $4_1^+ \rightarrow 2_1^+$  transitions of  $^{98}\text{Zr}$ . The 158.5 keV,  $2_1^+ \rightarrow 0_1^+$  transition of  $^{148}\text{Ce}$  has been used to generate the spectrum of figure 1(c). It is to be pointed out here that the fission fragment spectroscopy (FFS) measurement technique is based on the fact that the yield (or, total intensity) of the lowest  $2_1^+ \rightarrow 0_1^+$  ground state feeding transition, emitted during the de-excitation process, of an even-even fission fragment represents typically the yield of the concerned fission fragment [19]. In the present work, the yield measurements of the odd mass fission fragment nuclei were not considered due to the fact that the level schemes of the neutron-rich odd-mass nuclei are not known in detail for majority of the cases. It is also important to mention here that the yields of the fission fragments measured in the present work were corrected for the contaminations arising from (i) parallel side-feeding gamma transitions

to the ground state; (ii) internal conversion process; (iii) precursors' beta-decay contributions; and (iv) presence of low-lying millisecond, and/or microsecond isomers. The detailed prescription for the yield measurement following the FFS technique can be found in Ref.[12]. This measurement technique allows for the extraction of the correlated fragment yields between the lighter and heavier group of fragments by using cross gate conditions [12]. The correlated fragment yield distribution profiles obtained from both the experiments have been shown in figure 2. The observed peaks in the correlated fragment yield distributions are associated with the average neutron multiplicity value for  $^{236}\text{U}$  at  $E_{ex} = 6.5$  and  $21.5$  MeV, respectively. In case of the reaction,  $^{235}\text{U}(n_{th},f)$  the figure indicates that the maximum counts (peaks) are positioned at the coordinates  $(A_1, A_2) \sim (100, 134)$  and  $(90, 144)$ . These two peaks correspond to the average value of neutron multiplicity ( $\approx 2$  [20]) for  $^{236}\text{U}$  at  $E_{ex} = 6.5$  MeV. Similarly, the maximum counts (peaks) are positioned at the coordinates  $(A_1, A_2) \sim (98, 134)$  and  $(90, 142)$  for the reaction,  $^{232}\text{Th}(\alpha,f)$ . This is due to the fact that the average neutron multiplicity value for  $^{236}\text{U}$  at  $E_{ex} = 21.5$  MeV is  $\approx 4$  [16].

The measured relative isotopic yield distributions corresponding to the first and second experiments have further been utilized to extract the relative fission fragment mass yield distribution (FFMD) profiles for the compound nucleus,  $^{236}\text{U}$  at  $E_{ex} = 6.5$  and  $21.5$  MeV, respectively. The FFMD profile is generated by adding the measured raw yields of all the fission fragments corresponding to different  $Z$ -values, but having the same  $A$ -value. The experimental FFMDs obtained from the experiments are depicted in figure 3. The experimental results have further been interpreted on the basis of the Multi-Modal Random Neck Rupture Model (MM-RNRM) [4, 21]. It is to be noted here that although the relative mass yield distributions have been generated using only even- $Z$ , even- $N$  fission fragments, and not considering all the possible  $Z, N$  combinations, even then the ultimate fitted Gaussian parameters (peak position, width) does not seem to change in comparison to what one would expect from the fittings by incorporating all the possible fission fragment yield data points. This fact has been confirmed by performing the required fits with and without using complete set of fission yield data corresponding to the induced and spontaneous fission (SF) reactions,  $^{235}\text{U}(n,f)$  and  $^{252}\text{Cf}(SF)$ , respectively. For this exercise, the necessary data have been taken from the available fission yield database [16, 20]. The experimental FFMDs have been deconvoluted by using multiple Gaussian functions corresponding to different types of fission modes based on the MM-RNRM interpretation. The decomposition of the Super-long (SL) symmetric mode has been done (see figure 3(b)) by fitting a Gaussian function at  $A_{CN}/2$  with  $\sigma_M$  estimated from the empirical systematics based on the LDM (Liquid Drop Model) [22] (where  $A_{CN}$  denotes the mass number of the fissioning compound nucleus, and  $\sigma_M$  is the width of the corresponding Gaussian function). As can be seen from figure 3, the asymmetric components were simultaneously fitted with two Gaussian functions corresponding to asymmetric S1 and S2 fission modes persisting in each group of

**Table 1.** The relative contributions (%) of the different coexisting low-energy fission modes for the fissioning nucleus,  $^{236}\text{U}$  at different values of excitation energy ( $E_{ex}$ ).

Reaction	$E_{ex}$ MeV	Standard I (S1) (%)	Standard II (S2) (%)
$^{235}\text{U}(n_{th},f)$	6.5	$22.1 \pm 4.9$	$77.9 \pm 4.1$
$^{232}\text{Th}(\alpha,f)$	21.5	$14.6 \pm 3.7$	$85.4 \pm 3.8$

the lighter and heavier fragments. All the fitting parameters were kept free during the fit of the asymmetric peaks, except the area corresponding to each fission mode. The condition that area of a particular fission mode should be equal in both the lighter and heavier group of fragments has been used as the only constraint during the fitting procedure. Furthermore, the fitted peak values from the lighter and heavier group of fragments corresponding to a particular fission mode should follow the common condition that  $A_1 + A_2 + \langle v \rangle_{S1,S2} = 236$ . Here,  $A_{1,2}$  represent the peak values of Gaussian functions used for the respective lighter and heavier group of fragments belonging to one particular mode of fission, and  $\langle v \rangle_{S1,S2}$  are the average neutron multiplicities for the respective S1 and S2 modes. Following the experimental results obtained from both the experiments, the different fitted curves under the prescription of MM-RNRM have been explicitly shown in figure 3. Table 1 highlights the extracted values of the relative contributions of the different coexisting low-energy fission modes for  $^{236}\text{U}$  at different values of  $E_{ex}$ .

The varying profile of the relative contributions of S1 and S2 mode for  $^{236}\text{U}$  with increase in  $E_{ex}$  has been shown in figure 4. The General description of Fission (GEF) [23] calculations have been carried out to make theoretical estimations of the same relative contributions of S1 and S2 mode for  $^{236}\text{U}$ , and the calculated results are shown in figure 4. The predicted results based on the MM-RNRM are also shown in figure 4. These results have been taken from Ref.[5]. Interestingly, both the experimental data points, albeit two in number, and theoretical results from MM-RNRM as well as GEF model seems to indicate a similar oscillatory pattern in the low-energy fission region for  $^{236}\text{U}$ . An attempt has been made to fit the oscillatory pattern of relative yields with an appropriate polynomial function. A third-order polynomial function looks to be sufficient to fit reasonably the GEF model predicted data points. Following this, a third-order polynomial function is used to fit the experimental data points (black points) and theoretical data points of Ref.[5] (red points) (see figure 4(a,b)). It can be seen from figure 4(a) that the contribution of S1 mode is about to increase after  $E_{ex} \sim 22$  MeV unlike the predictions from Wahl's systematics [7]. However, additional data points need to be incorporated in figure 4(a,b) for establishing firmly the said oscillatory behavior, and for extracting the underlying issues related to fission dynamics.

## 4 Summary

The underlying dynamics of the low-energy fission modes in the fissioning compound nucleus,  $^{236}\text{U}$  have

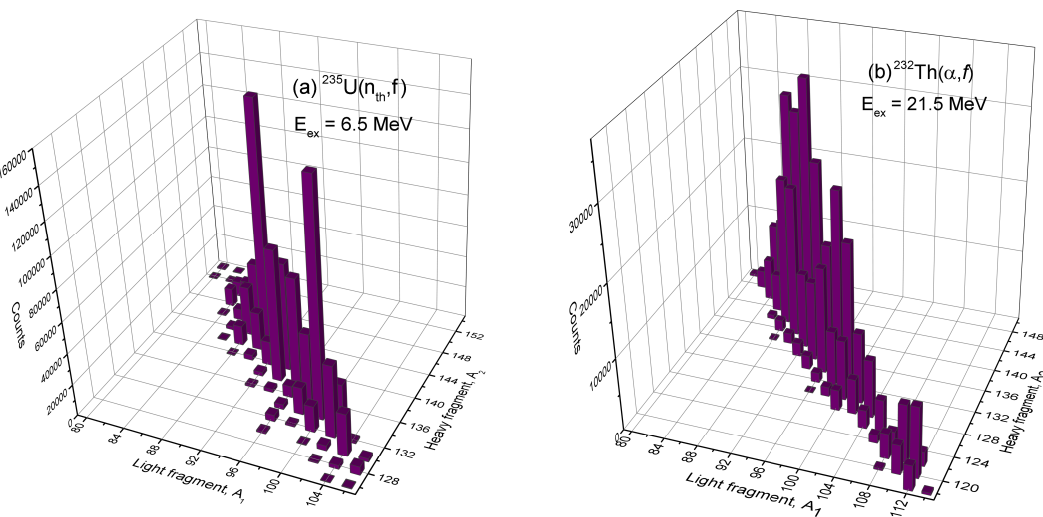


**Figure 2.** (a),(b): Correlated fragment yield distributions between the lighter and heavier group of fragment nuclei corresponding to the fissioning nucleus,  $^{236}\text{U}$  at  $E_{\text{ex}} = 6.5$  MeV and 21.5 MeV, respectively. See text for details.

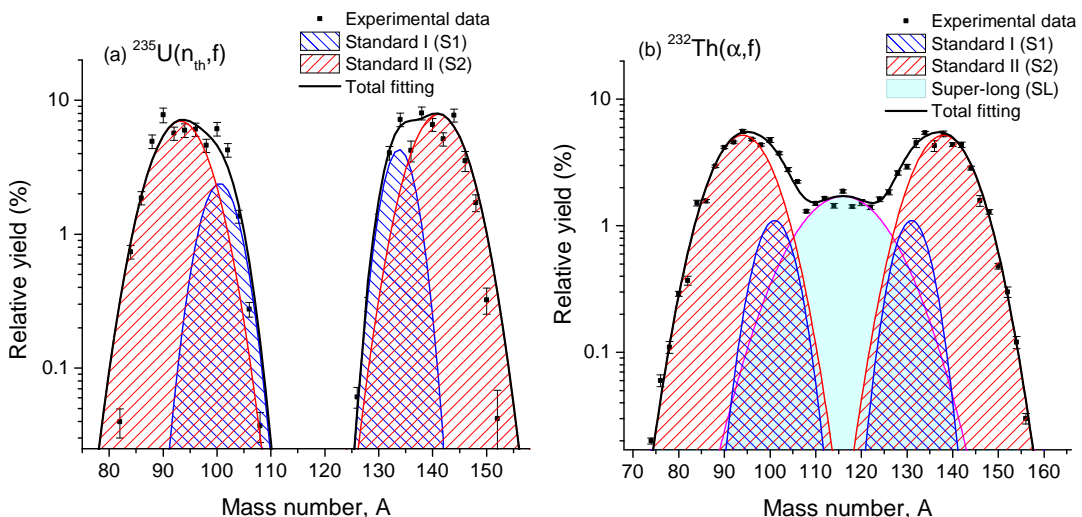


**Figure 3.** (a),(b): Relative fission fragment mass yield distribution of the fissioning compound nucleus,  $^{236}\text{U}$  produced from the reactions,  $^{235}\text{U}(n_{\text{th}},f)$  and  $^{232}\text{Th}(\alpha,f)$ , respectively. The experimental FFMDs have been fitted with multiple Gaussian functions corresponding to the different low-energy fission modes based on MM-RNRM formalism. See text for details.

been studied by employing the Fission Fragment Spectroscopy (FFS) technique. Correlated neutron rich fission-fragment nuclei produced in the reactions,  $^{235}\text{U}(n_{\text{th}},f)$  and  $^{232}\text{Th}(\alpha,f)$  have been investigated following prompt high-resolution  $\gamma$ -ray spectroscopy method. The  $\gamma\gamma$  and  $\gamma\gamma\gamma$  coincidence data have been analyzed to measure the relative isotopic yield distributions of the even-even fission fragments. These relative isotopic yield distributions were subsequently used for extracting the relative fission fragment mass yield distributions (FFMD) for the compound nucleus,  $^{236}\text{U}$  at  $E_{\text{ex}} = 6.5$  and 21.5 MeV, respectively. The analysis of the experimental FFMDs have been carried out by utilizing the concept of Multimodal Random Neck Rupture Model (MM-RNRM). The relative contributions of the two different types of asymmetric mode of fission, Standard I and Standard II have been investigated for  $^{236}\text{U}$  in the low-excitation regime ( $E_{\text{ex}} < 22$  MeV). The tentative evidence related to an oscillatory of varying pro-

file for the fission probabilities of different fission modes associated with the low-energy fission has been presented. The additional experimental data are required for drawing any firm conclusive evidence. In this context, the new experiments are being planned.

## 5 Acknowledgments

The authors are grateful to the entire EXILL collaboration especially U. Köster, A. Blanc, M. Jentschel, S. Leoni, P. Mutti, G. Simpson, and T. Soldner for their help and co-operation in performing the experiment at ILL. Help and support received from the reactor operation staffs at ILL, Grenoble related to our work with  $^{235}\text{U}(n_{\text{th}},f)$  reaction is gratefully acknowledged. The authors are also highly indebted to all the members of the VECC-INGA collaboration for their help and support at different stages of our work related to the fission reaction,  $^{232}\text{Th}(\alpha,f)$ . Two of

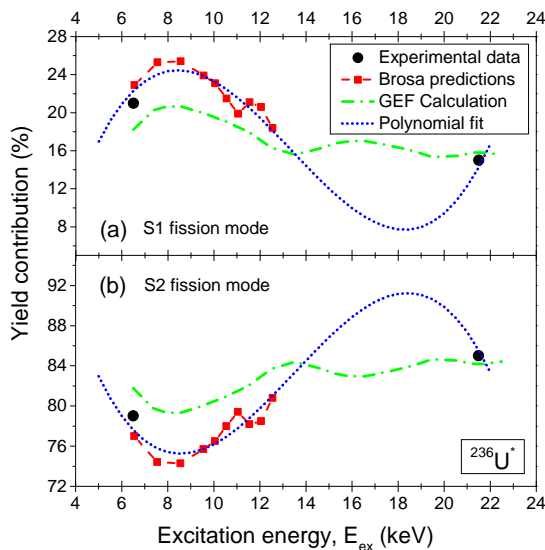


**Figure 4.** (a),(b): The correlation between the yield contribution probabilities (%) of different fission modes (S1 and S2) and excitation energy ( $E_{ex}$ ) of the fissioning compound nucleus,  $^{236}\text{U}$ . The experimental data points have been compared with two theoretical model calculations based on the (1) MM-RNRM [5] and (2) GEF [23]. The dotted blue lines represent polynomial fits to the experimental (black) and theoretical (red) data points. See text for details.

the authors (A.D. and A.C.) gratefully acknowledge the financial assistance received from the DAE-BRNS, Govt. of India (Project Sanction No.: 37(3)/14/17/2016-BRNS) for carrying out this work. One of the authors (A.C.) would also like to acknowledge the financial assistance received from Science and Engineering Research Board (SERB), Government of India (File Number: CRG/2021/004680), Inter-University Accelerator Centre (IUAC), New Delhi (Project Code No. UFR 71344), and UGC-DAE CSR (Project No.: CRS/2021-22/02/472).

## References

- [1] R. Vandenbosch and J.R. Huizenga, Nuclear Fission, Academic, New York, 1973
- [2] A. Turkevich and J. B. Niday, Phys. Rev. **84**, 52 (1951)
- [3] E. Konecny, H. J. Specht, and J. Weber, Phys. Lett. B **45**, 329 (1973)
- [4] U. Brosa, S. Grossmann, and A. Müller, Phys. Rep. **197**, 167 (1990)
- [5] U. Brosa, H. H. Knitter, T. Fan, J. Hu, and S. Bao, Phys. Rev. C **59**, 767 (1999)
- [6] S. S. Belyshev, B. S. Ishkhanov, A. A. Kuznetsov, and K. A. Stopani, Phys. Rev. C **91**, 034603 (2015)
- [7] A. C. Wahl, At. Data Nucl. Data Tables **39**, 1 (1988)
- [8] K. Hirose, K. Nishio, S. Tanaka, R. Leguillon, H. Makii, I. Nishinaka, R. Orlandi, K. Tsukada, J. Smallcombe, M. J. Vermeulen, S. Chiba, Y. Aritomo, T. Ohtsuki, K. Nakano, S. Araki, Y. Watanabe, R. Tatsuzawa, N. Takaki, N. Tamura, S. Goto, I. Tsekhanovich, and A. N. Andreyev, Phys. Rev. Lett **119**, 222501 (2017)
- [9] S. I. Mulgin, S. V. Zhdanov, N. A. Kondratiev, K. V. Kovalchuk, and A.Ya. Rusanov, Nucl. Phys. A **824**, 1 (2009)
- [10] F. Vives, F. J. Hambach, H. Bax, and S. Oberstedt, Nucl. Phys. A **662**, 63 (2000)
- [11] A. C. Berriman, D. J. Hinde, D. Y. Jeung, M. Dasgupta, H. Haba, T. Tanaka, K. Banerjee, T. Banerjee, L. T. Bezzina, J. Buete, K. J. Cook, S. Parker-Steele, C. Sengupta, C. Simenel, E. C. Simpson, M. A. Stoyer, B. M. A. Swinton-Bland, and E. Williams, Phys. Rev. C **105**, 064614 (2022)
- [12] Aniruddha Dey, D. C. Biswas, A. Chakraborty, S. Mukhopadhyay, A. K. Mondal, L. S. Danu, B. Mukherjee, S. Garg, B. Maheshwari, A. K. Jain, A. Blanc, G. de France, M. Jentschel, U. Köster, S. Leoni, P. Mutti, G. Simpson, and T. Soldner, C. A. Ur, and W. Urban, Phys. Rev. C **103**, 044322 (2021)
- [13] J. N. Wilson, D. Thisse, M. Lebois, N. Jovancević, D. Gjestvang, R. Canavan, M. Rudigier, D. Étasse, R-B. Gerst, L. Gaudefroy, E. Adamska, P. Adsley, A. Algora, M. Babo, K. Belvedere, J. Benito, G. Benzoni, A. Blazhev, A. Boso, S. Bottoni, M. Bunce, R. Chakma, N. Cieplińska-Orynczak, S. Courtin, M. L. Cortes, P. Davies, C. Delafosse, M. Fallot, B. Fornal, L. Fraile, A. Gottardo, V. Guadilla, G. Häfner, K. Hauschild, M. Heine, C. Henrich, I. Homm, F. Ibrahim, Ł. W. Iskra, P. Ivanov, S. Jazrawi, A. Korgul, P. Koseoglou, T. Kröll, T. Kurtukian-Nieto, L. Le Meur, S. Leoni, J. Ljungvall, A. Lopez-Martens, R. Lozeva, I. Matea, K. Miernik, J. Nemer, S. Oberstedt, W. Paulsen, M. Piersa, Y. Popovitch, C. Porzio, L. Qi, D. Ralet, P. H. Regan, K. Rezynkina, V. Sánchez-Tembleque, S. Siem, C. Schmitt, P-A. Söderström, C. Sürder, G. Tocabens, V. Vedia, D. Verney, N. Warr, B. Wasilewska, J. Wiederhold, M. Yavahchova, F. Zeiser, and S. Ziliani, Nature **590**, 566 (2021)
- [14] S. Leoni, C. Michelagnoli, and J. N. Wilson, La Rivista del Nuovo Cimento **45**, 461 (2022)
- [15] M. Jentschel, A. Blanc, G. de France, U. Köster, S. Leoni, P. Mutti, G. Simpson, T. Soldner, C. Ur, W. Urban, S. Ahmed, A. Astier, L. Augé, T. Back, P. Baczyk, A. Bajoga, D. Balabanski, T. Belgya, G. Benzoni, C. Bernards, D. C. Biswas, G. Bocchi, S. Bottoni, R. Britton, B. Bruyneel, J. Burnett, R. B. Cakirli, R. Carroll, W. Catford, B. Cederwall, I. Celikovic, N. Cieplińska-Orynczak, E. Clement, N. Cooper, F. Crespi, M. Csatlos, D. Curien, M. Czerwinski, L. S. Danu, A. Davies, F. Didierjean, F. Drouet, G. Duchene, C. Ducoin, K. Eberhardt, S. Erturk, L.M. Fraile, A. Gottardo, L. Grente, L. Grocott, C. Guerrero, D. Guinet, A. L. Hartig, C. Henrich, A. Ignatov, S. Ilieva, D. Ivanova, B. V. John, R. John, J. Jolie, S. Kishev, M. Krticka, T. Konstantinopoulos, A. Korgul, A. Krasznahorkay, T. Kröll, J. Kurpeta, I. Kuti, S. Lalkovski, C. Larijani, R. Leguillon, R. Lica, O. Litaize, R. Lozeva, C. Magon, C. Mancuso, E. Ruiz Martinez, R. Massarczyk, C. Mazzocchi, B. Melon, D. Mengoni, C. Michelagnoli, B. Million, C. Mokry, S. Mukhopadhyay, K. Mulholland, A. Nannini, D. R. Napoli, B. Olaizola, R. Orlandi, Z. Patel, V. Paziy, C. Petrache, M. Pfeiffer, N.

Pietralla, Z. Podolyak, M. Ramdhane, N. Redon, P. Regan, J. M. Regis, D. Regnier, R. J. Oliver, M. Rudigier, J. Runke, T. Rzaca-Urban, N. Saed-Samii, M. D. Sal-sac, M. Scheck, R. Schwengner, L. Sengele, P. Singh, J. Smith, O. Stezowski, B. Szpak, T. Thomas, M. Thürauf, J. Timar, A. Tom, I. Tomandl, T. Torny, C. Townsley, A. Tuerler, S. Valenta, A. Vancraeyenest, V. Vandone, J. Vanhoy, V. Vedia, N. Warr, V. Werner, D. Wilmsen, E. Wilson, T. Zerrouki, and M. Zielinska, *JINST* **12**, P11003 (2017)

[16] Aniruddha Dey, D. C. Biswas, A. Chakraborty, S. Mukhopadhyay, A. K. Mondal, K. Mandal, B. Mukherjee, R. Chakrabarti, B. N. Joshi, L. A. Kinage, S. Chatterjee, S. Samanta, S. Das, Soumik Bhattacharya, R. Banik, S. Nandi, Shabir Dar, R. Raut, G. Mukherjee, S. Bhattacharyya, and A. Goswami, *Phys. Lett. B* **825**, 136848 (2022)

[17] D. C. Radford, *Nucl. Instrum. Meth. Phys. Res., Sect. A* **361**, 297 (1995)

[18] J. Theuerkauf, *Tv Software package*, <http://www.ikp.uni-koeln.de/~fitz/>

[19] E. Cheifetz, J. B. Wilhelmy, R. C. Jared, and S. G. Thompson, *Phys. Rev. C* **4**, 1913 (1971)

[20] T.R. England and B.F. Rider, *ENDF/B-VII.1 LA-UR-94-3106*, <https://doi.org/10.2172/10103145>

[21] Aniruddha Dey *et al.*, Manuscript under preparation

[22] G. N. Knyazheva, E. M. Kozulin, R. N. Sagaidak, A. Yu. Chizhov, M. G. Itkis, N. A. Kondratiev, V. M. Voskressensky, A. M. Stefanini, B. R. Behera, L. Corradi, E. Fioretto, A. Gadea, A. Latina, S. Szilner, M. Trotta, S. Beghini, G. Montagnoli, F. Scarlassara, F. Haas, N. Rowley, P. R. S. Gomes, and A. Szanto de Toledo, *Phys. Rev. C* **75**, 064602 (2007)

[23] K. H. Schmidt, B. Jurado, C. Amouroux, and C. Schmitt, *Nucl. Data Sheets* **131**, 107 (2016)